UCRL--93829

DE86 005177

THEORY AND ANALYSIS OF SOFT X-RAY LASER EXPERIMENTS

Barbara L. Whitten
Andrew U. Hazi
Lawrence Livermore National Laboratory
University of California
Livermore, CA 94550

This paper was prepared for submittal to the
7th International Workshop on Laser Interaction
and Related Plasma Phenomena, Monterey, CA

October/November 1985

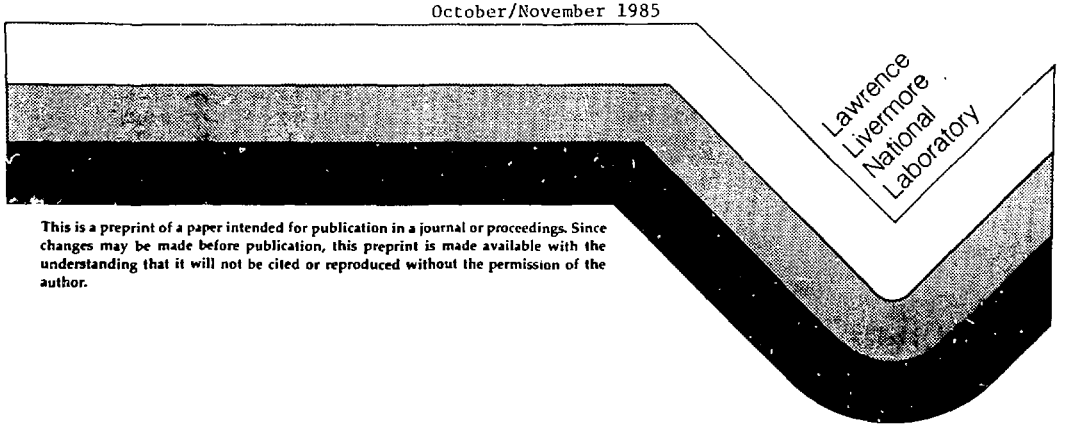

THEORY AND ANALYSIS OF SOFT X-RAY LASER EXPERIMENTS

Barbara L. Whitten and Andrew U. Hazi

University of California, Lawrence Livermore National Laboratory
Livermore, California 94550

ABSTRACT

The atomic modeling of soft x-ray laser schemes presents a formidable challenge to the theorists -- a challenge magnified by the recent successful experiments. A complex plasma environment with many ion species present must be simulated. Effects such as turbulence, time dependence, and radiation transport, which are very difficult to model accurately, may be important. We shall describe our efforts to model the recently demonstrated soft x-ray laser in collisionally pumped neon-like selenium, with emphasis on the ionization balance and excited state kinetics. The relative importance of various atomic processes, such as collisional excitation and dielectronic recombination, on the inversion kinetics will be demonstrated. We shall compare our models with experimental results and evaluate the success of this technique in predicting and analyzing the results of x-ray laser experiments.

INTRODUCTION

The recent demonstration of amplified spontaneous emission (ASE) in neon-like selenium[1] was highly successful from an experimental point of view. Many questions remain, however, about the nature of the dense, laser-produced plasma in which ASE took place. Some of these questions are theoretical in nature, and some are experimental, requiring further and more refined measurements of the plasma.

The purpose of this paper is to describe some important questions about the neon-like selenium x-ray laser (XRL) plasma. We shall describe the work done so far, the present state of our knowledge, and the work we are planning. We shall concentrate on three major areas: plasma characterization, ionization balance, and excited state kinetics.

Before we begin, an important distinction must be made. Theoretical and computational work at Livermore can be divided into two broad categories. The first is design, which uses large simulation codes to model the complex interaction between the optical laser light and the target. At Livermore, the well-known hydrodynamics code LASNEX[2] is used to model the laser-plasma interaction, the subsequent hydrodynamics, and gross radiation output. Then the x-ray laser design code XRASER[3] takes the hydrodynamic output from LASNEX and models the ionization balance and detailed level populations to produce gain coefficients, synthetic spectra, and other atomic physics information. This approach is essential to the laboratory x-ray laser program, since it is used for target design, as well as analysis of integral target experiments. This work is carried on by Peter Hagelstein, the author of XRASER, and Mordy Rosen and his group.

The second approach taken by theorists is to use smaller, more specialized codes to analyze particular parts of a problem, or to compare with specially designed experiments. Because these codes do not attempt to simulate the many complex interactions that occur in laser-generated plasmas, they are clearly less general than the large scale design codes. However, they are also smaller, cheaper to run, and easier to modify. This is the approach described in this paper.

(a)

1a. Typical laser interferogram of exploding foil plasma during irradiation by CHROMA laser at KMS Fusion, Inc.

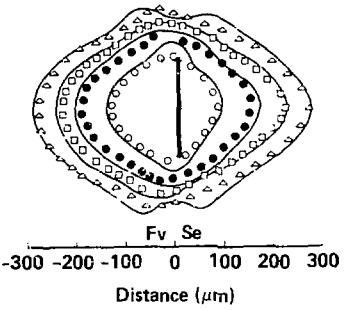

(b)

1b. Comparison of density profiles obtained from laser interferometry to predictions of LASNEX.
Experiment: o 2×10^{20},
● 1×10^{20},
□ 5×10^{19},
△ 2×10^{19},
Theory: – LASNEX.

PLASMA CHARACTERIZATION

In this section we describe our attempts to characterize the selenium plasma. We shall concentrate on the determination of the electron temperature and density, although there are other important plasma parameters.

Our general approach has been to measure these quantities in specially designed experiments performed at KMS Fusion, Inc. The results are then used to verify LASNEX predictions of the plasma parameters.

The electron density is measured using the technique of laser interferometry.[4] An exploding foil target is irradiated by frequency-doubled neodymium-glass laser light to produce conditions appropriate to the x-ray laser plasma. The plasma is probed by a short laser pulse and an interferogram is formed. This is Abel inverted to produce density contours. Figure 1 shows a typical interferogram, and the density contours produced. Also shown are predictions[1] of the density contours from LASNEX. Clearly, the agreement is very good.

Because the experimental technique is well developed, and because there is agreement between measurements and LASNEX predictions, we regard this method as satisfactory. Future work will use the more advanced four-frame holography technique to look at more complex targets. Some of this work is described in the paper by George Cheratis[5] in this volume.

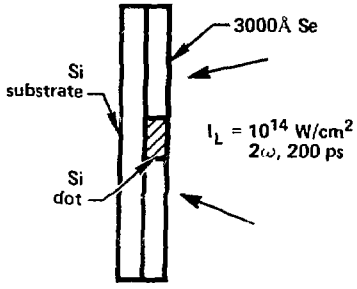

(a)

2a. Diagram of target used for silicon dot experiments at KMS Fusion, Inc. to determine plasma temperature from Lyman alpha to helium alpha line ratio.

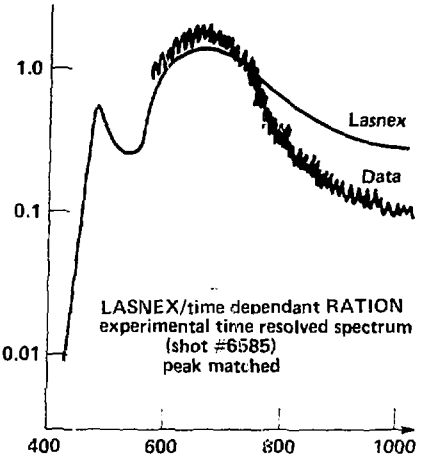

(b)

2b. Lyman alpha to helium alpha line ratio versus time for LASNEX prediction and for experimental time resolved spectrum. The time of the peaks are matched.

The electron temperature is measured using silicon dot spectroscopy. The target is a slab of silicon coated with a thin layer of selenium, on which a dot of silicon 100 microns in diameter is left exposed. When this target is irradiated, the selenium emits L-shell lines, and the silicon emits K-shell lines in the same spectral region. The ratio of the Lyman alpha line of hydrogenic silicon to the $2p\,^1P - 1s\,^1S$ resonance line of helium-like silicon is used as a temperature diagnostic. Because this ratio is not in steady state at the XRL plasma conditions, LASNEX is used to drive a time-dependent version of the K-shell spectroscopy code RATION.[6]

Figure 2 shows a diagram of the target, together with the results. The predicted line ratio agrees with the experimental result very well during the peak of the laser pulse. Unfortunately, a number of effects, such as overlap between selenium and silicon lines in the experimental data, opacity, and a small amount of data conspire to make this result considerably less reliable than the density measurement. In addition, since these experiments so far have been done with slab targets rather than exploding foils, the results only indirectly confirm the calculated temperature for XRL targets. We also measure the electron temperature using the short wavelength cutoff of Raman scattering.[7] The two methods are in good agreement, but neither is particularly accurate.

Because we currently have no simple and accurate measure of the temperature, future work will concentrate on evaluating alternative temperature diagnostics. We plan to compare, at the plasma conditions typical of the XRL plasma, the slope of the continuum radiation, the

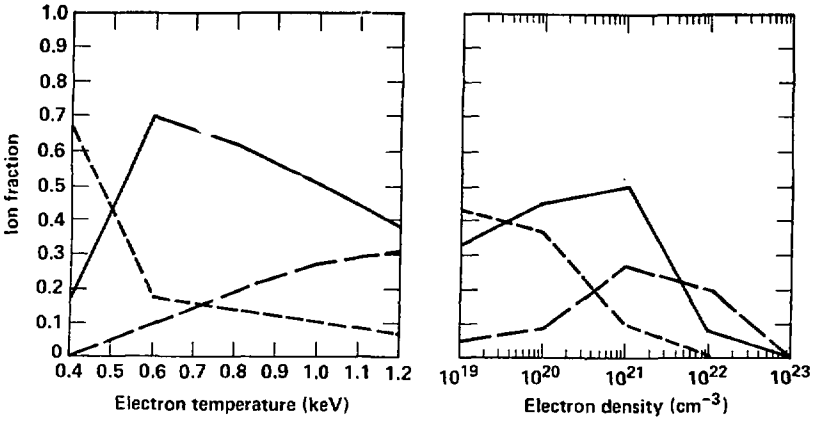

(a) (b)

3a. Fraction of sodium-like, neon-like, and fluorine-like ions versus electron temperature for $n_e = 10^{21}$ cm^{-3}.

3b. Fraction of sodium-like, neon-like, and fluorine-like ions versus electron density for T_e = 1000 eV.

Ion fractions are calculated using a steady-state scaled hydrogenic model.
Short dash - sodium-like ions,
Solid line - neon-like ions,
Long dash - fluorine-like ions.

Lyman alpha/helium alpha line ratio, and the lithium-like satellite lines. In addition, we are investigating the possibility of direct L-shell temperature diagnostics.

IONIZATION BALANCE

We now turn to the kinetics of the selenium plasma itself. This is a formidable modeling problem involving many ionization stages, each with complex atomic structure. Fortunately, the problem can be separated into two rather distinct parts. The first is the determination of the distribution of ion species in the plasma. The second is the study of detailed excited state kinetics for neon-like and nearby ions, which will be discussed in the next section.

To model the ionization balance, we need to construct an atomic model which contains a large number of ionization stages, and a large number of energy levels (measured by principle quantum number) for each ionization stage. However, it is probably not necessary to include detailed atomic physics. This is because ionization balance is largely controlled by ionization and recombination between the high Rydberg states and the next ionization continuum. For these states, the excited electron is rather hydrogenic in character.

For preliminary estimates of the ionization balance, we used the steady state, scaled hydrogenic code of Y. T. Lee,[8] which contains the

ten ionization stages nearest the most probable, and ten Rydberg states for each stage. Figure 3 shows that neon-like ions dominate for plasma conditions similar to those of the selenium XRL plasma (which are determined to be n_e = 3-5 x 10^{20} cm^{-3} and T_e = 1 keV by the methods described in the previous section).

These results are qualitatively confirmed by time-resolved spectra of the 3-2 emission for selenium obtained during the XRL experiments by a streaked x-ray crystal spectrometer. These show strong neon-like and fluorine-like emission.

However, both theoretical and experimental problems make more quantitative comparisons difficult. First, time-dependent calculations indicate that the ionization balance is not in steady state. Time dependant calculations are more difficult, and at present different calculations are not in agreement,[9] making quantitative predictions uncertain. Secondly, experimental evidence about the ionization balance is spectroscopic in nature, which gives direct information only about excited state abundances. Since most of the population of neon-like and fluorine-like ions is in the ground state, this evidence is of limited usefulness.

We plan in the future to improve both modeling and experimental techniques. We shall investigate different time-dependent codes to determine the source of the discrepancies. We also plan to investigate the importance of effects not presently included in calculations, for example, higher order processes like dielectronic recombination, radiation trapping, the role of higher Rydberg states and the effects of external fields, i.e., plasma microfields or time-dependent fields due to the optical pump laser.

Experimentally, we plan to obtain time-dependent 3-2 spectra at high spectral resolution, which will give us more detailed information about ion abundances, albeit still of excited states only. Ultimately, we wish to do absorption experiments, which will give us ground state populations directly.

EXCITED STATE KINETICS

This is the complementary part of the ionization balance problem discussed in the previous section. In this case, we are interested only in neon-like ions, or those of nearby ionization stages. However, we wish to obtain detailed populations of each excited state. This information is then used to obtain line intensities, line ratios, and gain coefficients, for comparison with experiment.

Because the atomic physics used in detailed kinetic models has a major influence on the results, we shall spend some time describing the atomic physics of our model. Most calculations described in this section were done using a 92-level model, which includes the $2s^22p^6$ (J = 0) neon-like ground state, the 36 n = 3 and the 52 n = 4 excited states, and the three fluorine-like states $2s^22p^5$ (J = 1/2, 3/2) and $2s2p^6$ (J = 1/2). Energies and radiative rates were computed using configuration interaction wave functions in intermediate coupling. For the n = 2 and n = 3 states of Ne-like selenium, we used the atomic structure code SUPERSTRUCTURE,[10] for the n = 4 states of Ne-like ion and the F-like states, we used the multiconfigurational Dirac-Fock code YODA.[11]

All collisional excitation rates were calculated by averaging collision strengths over a Maxwellian electron distribution. For the

n = 2-3 transitions, the distorted wave code DSW[12] was used to compute L-S scattering amplitudes, which were transformed to intermediate coupling using JAJOM.[13] The n = 2-4 collision strengths were calculated directly in intermediate coupling using the relativistic distorted wave code MCDW.[11] The collision strengths for the electric dipole allowed, excited state-excited state transitions in the Ne-like ion, and the 2s-2p transitions in the F-like ion, were calculated using the classical path method.[14] Finally, the collision strengths for transitions among the fine-structure levels of a given n = 3 configuration [e.g., $(2p^5 3p)\ J \rightarrow 2p^5 3p\ J']$ were computed with DSW and JAJOM.

Ionization and three-body recombination rates were calculated using the scaled hydrogenic rates of Sampson and coworkers.[15] Radiative recombination rates were obtained using the prescription of Weisheit, et al.[16] All these rates are given by simple formulae which do not take into account the detailed structure of the states.

At the plasma conditions described above, the dominant recombination process is dielectronic recombination, which we treated in full detail for all the $(3\ell 3\ell')$ and $(3\ell 4\ell')$ doubly excited states of Ne-like selenium. The dielectronic recombination coefficients were calculated in the isolated resonance approximation.[17] The Auger and radiative rates of the individual doubly excited states were evaluated in intermediate coupling with configuration interaction using the multi-configuration Dirac-Fock method.[17,18]

Tables 1 and 2 contain typical results. Table 1 gives the energies of some important levels, together with the rate coefficients for ionization from and recombination into these levels. Table 2 contains radiative decay rates and collisional excitation rate coefficients for some relevant transitions. All these results are given for the selenium XRL plasma conditions described above.

The kinetic model constructs rate equations and solves them in steady state for the level populations. The relative inversion density for a particular transition is given by:

$$y_{UL} = \nu_U - g_U \nu_L / g_L,$$

where ν_U (ν_L) and g_U (g_L) are the relative population and statistical weight, respectively, of the upper (lower) state of the transition. (Relative population is defined as the fraction of neon-like ions in a particular excited state.) The gain coefficient of a Doppler broadened line is given by the expression:

$$\alpha = \frac{\lambda^3 A}{8\pi} \left[\frac{M_i}{2\pi k T_i}\right]^{1/2} y_{UL}\, n_{Ne}$$

where λ and A are the wavelength and radiative decay rate, respectively, of the lasing transition, M_i and T_i are the mass and temperature, respectively, of the ion, and n_{Ne} is the total density of Ne-like ions. We have taken the plasma parameters for these calculations to be those characteristic of the neon-like selenium laser plasma:[1] $n_e = 5 \times 10^{20}$ cm^{-3}, $T_e = 1000$ eV, $T_i = 400$ eV, and $n_{Ne} = 5 \times 10^{18}$ cm^{-3}. The fraction of Ne-like ions is assumed to be 0.25.

It should be emphasized that this simple model can not be expected to provide accurate gains which can be compared to experiment. Because important effects like time-dependance, radiation trapping and laser loss

Table 1. Energies relative to the neon-like ground state (eV), and ionization and recombination rate coefficients ($cm^3 sec^{-1}$) for some levels of neon-like selenium. All rate coefficients are given for T_e = 1000 eV.

Level	Energy	Collisional Ionization	Radiative Recombination	Dielectronic Recombination
$2p^5 3s$ (J=1)[a]	1438.5	2.20^{-11}	1.74^{-14}	3.02^{-14}
$2p^5 3s$ (J=1)[b]	1480.9	2.20^{-11}	1.74^{-14}	2.40^{-14}
$2p^5 3s$ (J=2)[c]	1499.4	2.51^{-11}	2.77^{-14}	7.17^{-14}
$2p^5 3p$ (J=2)[d]	1540.9	2.51^{-11}	2.78^{-14}	7.60^{-14}
$2p^5 3p$ (J=0)[e]	1549.5	2.51^{-11}	5.52^{-15}	1.94^{-14}
$2p^5 3d$ (J=3)	1607.8	3.03^{-11}	3.68^{-14}	8.48^{-14}

[a]Lower level of 206.4Å laser transition.
[b]Lower level of 209.8Å and 182.4Å laser transition.
[c]Upper level of 206.4Å laser transition.
[d]Upper level of 209.8Å laser transition.
[e]Upper level of 182.4Å laser transition.

Table 2. Calculated transition energies, radiative decay rates (sec^{-1}), and collisional excitation rate coefficients ($cm^3\ sec^{-1}$) at T_e = 1000eV for some transitions of neon-like selenium.

Upper state	Lower state	Transition Energy	Radiative Decay	Collisional Excitation
$2p^5 3s$ (J=1)	$2p^6$ (J=0)	1438.5[a]	4.16^{12}	8.53^{-13}
$2p^5 3s$ (J=1)	$2p^6$ (J=0)	1480.9[b]	2.89^{12}	6.19^{-13}
$2p^5 3p$ (J=2)	$2p^6$ (J=0)	1499.4	4.66^{9}	8.39^{-13}
$2p^5 3p$ (J=2)	$2p^6$ (J=0)	1540.9	5.14^{9}	9.39^{-13}
$2p^5 3p$ (J=0)	$2p^6$ (J=0)	1549.5	------	1.06^{-11}
$2p^5 3d$ (J=3)	$2p^6$ (J=0)	1607.8	------	9.75^{-13}
$2p^5 3p$ (J=2)	$2p^5 3s$ (J=1)	60.9[c]	7.96^{9}	7.47^{-10}
$2p^5 3p$ (J=2)	$2p^5 3s$ (J=1)	60.0[d]	1.54^{9}	1.52^{-9}
$2p^5 3p$ (J=0)	$2p^5 3s$ (J=1)	68.6[e]	2.47^{10}	2.80^{-10}
$2p^5 3d$ (J=3)	$2p^5 3p$ (J=2)	66.9	1.92^{10}	1.08^{-9}

[a]Dump line for 206.4Å laser transition.
[b]Dump line for 209.8Å and 182.4Å laser transitions.
[c]206.4Å laser transition.
[d]209.8Å laser transition.
[e]182.4Å laser transition.

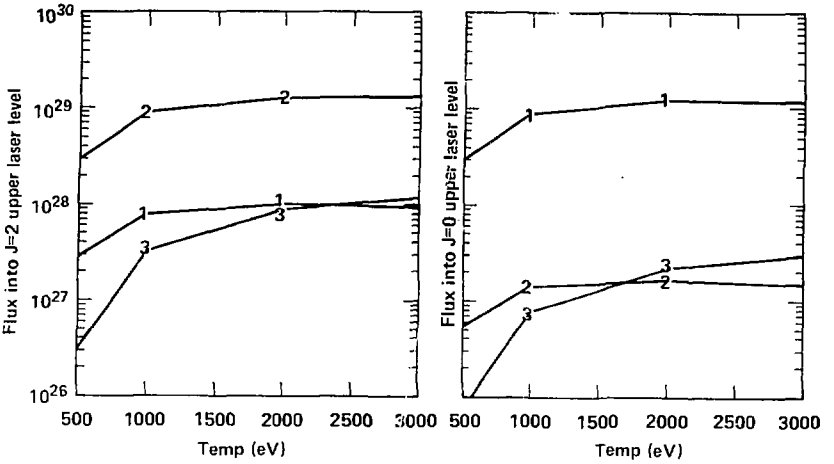

4a. Flux (cm^{-3} sec^{-1}) into upper state of 206.4 Å (J=2-1) laser transition versus electron temperature for $n_e = 5 \times 10^{20}$ cm^{-3}.

4b. Flux (cm^{-3} sec^{-1}) into upper state of 182.4 Å (J=0-1) laser transition versus electron temperature for the same density.

1 - Collisional excitation from neon-like ground state,
2 - Collisional cascade from higher neon-like excited states,
3 - Dielectronic recombination from fluorine-like ground states.

mechanisms have been neglected, the gains obtained should be considered to be qualitative only.

This model has been used for extensive kinetics calculations relevant to the neon-like selenium x-ray laser. We shall describe some of the results which relate to one of the major theoretical puzzles revealed by the experiment.[1] Prior to the experiment, all theoretical work[19] predicted very high gain for one particular $2p^53p - 2p^53s$ (J = 0-1) transition at 182.4 A, which did not show significant amplification in the experiment. The lines that were observed resulted from two $2p^53p - 2p^53s$ (J = 2-1) transitions at 206.4 Å and 209.8 Å. This discrepancy between experiment and theory has not yet been satisfactorily explained.

It was initially believed that the principal population mechanism for all the $2p^53p$ upper states was collisional excitation from the ground state. Initial calculations therefore included only the ground state and n = 3 excited states of the neon-like system. It has become clear, however, that this is not sufficient to describe the kinetics of neon-like selenium. A possible explanation of the discrepancy between experiment and theory has been proposed by Apruzese et al.,[20] who suggest that the J = 2 - 1 transitions are pumped by radiative recombination from the fluorine-like ions at a relatively low electron temperature which results from very rapid radiative cooling of the plasma. However, more recent work[21] suggests that dielectronic recombination is the most important recombination mechanism at the plasma conditions ($n_e = 3\text{-}5 \times 10^{20}$ cm^{-3} and $T_e = 1$ keV) deduced from the plasma characterization experiments described in the previous section.

Table 3. Effects of n = 4-3 cascades and dielectronic recombination on gain coefficients (cm^{-1}) of some $2p^53p - 2p^53s$ transitions in neon-like selenium, at the following plasma conditions: $n_e = 5 \times 10^{20}$ cm^{-3}, $T_e = 1000$ eV, $T_i = 400$ eV, and $n_i = 5 \times 10^{18}$ cm^{-3}.

Transition	Wavelength (Å)	No Cascade or Recombination	Cascade Only	Recombination Only	Cascade and Recombination
J = 0 - 1	182.4	14.3	13.4	13.9	13.0
J = 2 - 1	209.8	11.4	13.0	13.8	15.3
J = 2 - 1	206.4	9.7	11.5	12.1	13.6

An examination of Tables 1 and 2 shows some important differences between the $2p^53p$ (J=0) and J=2) states. The $2p^53p$ (J=0) state is indeed populated primarily by a very large collisional excitation rate from the ground state, and the dielectronic recombination rate into this state is relatively small. For the $2p^53p$ (J=2) states, however, the collisional excitation rates are smaller, and dielectronic recombination from the fluorine-like ion and cascade from higher lying neon-like levels are at least as important as collisional excitation. This is further illustrated in Figure 4. Table 3 shows the changes in the calculated gain coefficients which result from adding these processes to the kinetic model. Figure 5 shows the gain of all seven possible $2p^53p - 2p^53s$ laser transitions as a function of the fluorine-like to neon-like ion ratio.

It is clear from this discussion that collisional cascade and dielectronic recombination are important processes, and must be included in any accurate description of the kinetics. It is also clear that they do not alone explain the discrepancy between theoretical prediction and the experimental result. The gain of the J = 0 - 1 transition has been reduced relative to that of the J = 2 - 1 transitions, but not by enough to explain the experimental results.

Our current theoretical work concentrates on mechanisms which will reduce the gain for all the laser transitions, such as bound-free absorption. Another possibility is resonance contributions to the collision rates, which can significantly increase the $2p^6 \rightarrow 2p^53s$ collisional excitation rates.[12] We shall also investigate additional population mechanisms for the J = 2 upper states, such as inner-shell ionization from sodium-like ions, or radiation trapping of the 3d-2p lines.

In addition, the Livermore team is planning to do experiments which will determine where in the plasma the x-ray ASE occurs, what the plasma conditions and ionization balance are, and what is the timing of the x-ray ASE relative to the optical laser pulse.

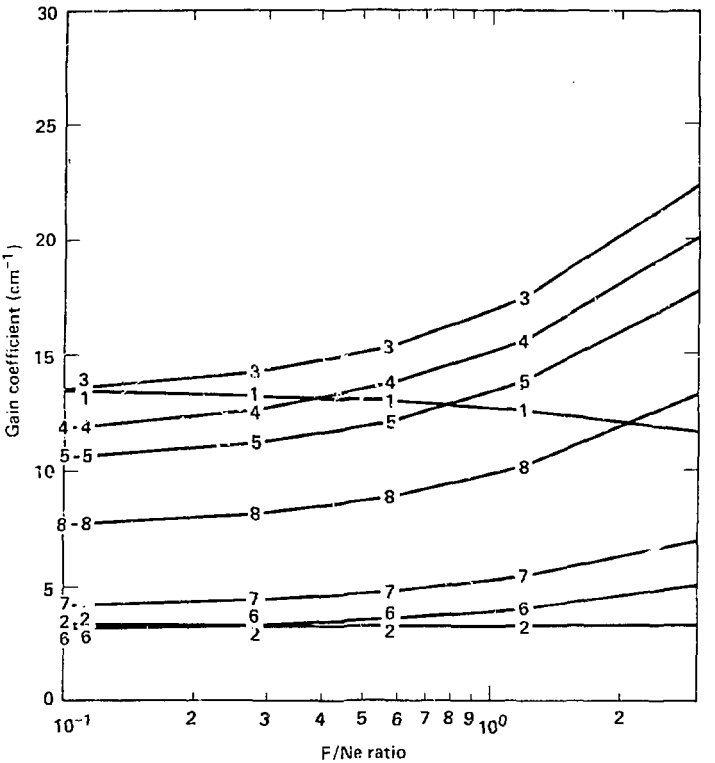

5. Gain coefficient (cm^{-1}) for the seven possible $2p^5 3p - 2p^5 3s$ laser transitions as a function of fluorine-like/neon-like ions. Gain coefficients are calculated using the 92-level model described in the text, and the following plasma conditions: $n_e = 5 \times 10^{20}$ cm^{-3}, T_e = 1000 eV, T_i = 400 eV, and $n_{Ne} = 10^{18}$ cm^{-3}.

1 - J = 0 - 1 transition at 182.4 A,
2 - J = 0 - 1 transition at 168.5 A,
3 - J = 2 - 1 transition at 206.4 A,
4 - J = 2 - 1 transition at 209.8 A,
5 - J = 2 - 1 transition at 262.9 A,
6 - J = 1 - 1 transition at 213 A,
7 - J = 1 - 1 transition at 261 A,
8 - J = 1 - 1 transition at 220.2 A.

CONCLUSIONS

The experiments in the summer of 1984 were highly successful, and the experimentalists are justly proud of their work. In a series of well-planned and extremely well-diagnosed experiments, the first incontrovertible evidence of ASE at soft x-ray wave lengths was obtained. For the theorists involved, however, the experiments raised as many questions as they answered. We have summarized here some of the outstanding questions which remain to be answered in the fields of plasma characterization, ionization balance, and excited state kinetics. For each category, we have described our present state of knowledge and the plans we have to further study each problem, both through theory and experiment.

ACKNOWLEDGMENT

The authors gratefully acknowledge the contributions of Dr. Dennis Matthews and the other members of the x-ray laser team at Livermore, and the spectroscopy team from KMS Fusion, Inc. This work was performed under the auspicies of the U.S. Department of Energy by the Lawrence Livermore National Laboratory under contract number W-7405-ENG-48.

REFERENCES

1. D. L. Matthews et al., Phys. Rev. Letters 54:110 (1985); M. D Rosen, et al., Phys. Rev. Letters 54:106 (1985).
2. G. B. Zimmerman, Lawrence Livermore National Laboratory Report No. UCRL-75881, 1974 (unpublished); G. B. Zimmerman and W. L. Kruer, Comments Plasma Phys. Controlled Fusion 2:85 (1975).
3. P. L. Hagelstein, Plasma Phys. 25:1345 (1983).
4. Gar. E. Busch, C. L. Shepard, L. D. Siebert, and J. A. Tarvin, Rev. Sci. Instrum. 56:879 (1985).
5. G. Charatis, Gar. E. Busch, C. L. Shepard, and M. D. Rosen, "Hydrodynamic Aspects of X-ray Laser Targets, 7th International Workshop on Laser Interaction and Related Plasma Phenomena, Monterey, CA, October, 1985.
6. R. W. Lee, B. L. Whitten, and R. E. Strout, J. Quant. Spectrosc. Radiat. Transfer 37:91, (1984); D. L. Matthews, et al., Appl. Phys. Letters 45:226 (1984).
7. R. E. Turner, et al., Phys. Rev. Lett. 54:189 (1985).
8. Y. T. Lee, "A Model for Ionization Balance and L-shell Spectroscopy of Non-equilibrium Plasmas," submitted to J. Quant. Spectrosc. Radiat. Transfer.
9. Y. T. Lee, "*TDIB-a Time Dependent Ionization Balance Code for non-LTE* Plasmas," 3rd International Conference on Radiative Properties of Hot Dense Matter", Williamsburg, VA. October 1985; R. S. Walling, P. L. *Hagelstein*, and Y. T. Lee, private communication.
10. W. Eissner, M. Jones, and H. Nussbaumer, Comp. Phys. Commun. 8:270 (1974).
11. P. L. Hagelstein, Ph. D. thesis, Lawrence Livermore National Laboratory No. UCRL-53100, 1981; P. L. Hagelstein and R. Jung, unpublished.
12. W. Eissner and M. J. Seaton, J. Phys. B 5:2187 (1972).
13. H. E. Saraph, Computer Phys. Comm. 1:232 (1970); H. E. Saraph, Computer Phys. Comm. 3:256 (1972).
14. A. Burgess and H. P. Summers, Mon. Not. Roy. Astr. Soc. 174:345 (1976).
15. D. L. Moores, L. B. Golden, and D. H. Sampson, J. Phys. B 13:385 (1980); L. B. Golden and D. H. Sampson, J. Phys. B 13:2645 (1980), and references therein.

16. J. C. Weisheit, C. B. Tarter, J. H. Scofield, and L. M. Richards, J. Quant. Spectrosc. Rad. Transfer 16:659 (1976).
17. M. H. Chen, submitted to Phys. Rev. A.
18. M. H. Chen, Phys. Rev. A 31:1449 (1985).
19. A. V. Vinogradov and V. N. Shlyaptsev, Sov. J. Quantum Elec. 10:754 (1980); and references therein; U. Feldman, A. K. Bhatia, and S. Suckewer, J. Appl. Phys. 54:2188 (1983); U. Feldman, J. F. Seely, and A. K. Bhatia, J. Appl. Phys. 56:2475 (1984).
20. J. P. Apruzese, J. Davis, M. Blaha, P. C. Kappel, and V. L. Jacobs, Phys. Rev. Lett. 55:1820 (1985).
21. B. L. Whitten, A. U. Hazi, M. H. Chen, and P. L. Hagelstein, "Effect of Dielectronic Recombination on the Kinetics of Neon-like Selenium", to be published in Phys. Rev. A, 1986.
22. G. A. Doschek, U. Feldman, and J. F. Seely, J. Appl. Phys. 58:3984 (1985).

DISCLAIMER